Experimental and quantum-chemical characterization of heavy carbon subchalcogenides: Infrared detection of SeC$_3$Se*

Thomas Salomon[a], John B. Dudek[b], Yury Chernyak[b], Jürgen Gauss[c], Sven Thorwirth[a,*]

[a]*I. Physikalisches Institut, Universität zu Köln, Zülpicher Str. 77, 50937 Köln, Germany*
[b]*Department of Chemistry, Hartwick College, Oneonta, NY, USA*
[c]*Department Chemie, Johannes Gutenberg-Universität Mainz, Duesbergweg 10-14, 55128 Mainz, Germany*

Abstract

High-resolution infrared studies of laser ablation products from carbon-selenium targets have revealed a new vibrational band at $2057\,\mathrm{cm^{-1}}$ that is identified as the ν_3 vibrational fundamental of the SeC$_3$Se cluster. Because of the rich isotopic composition of selenium and the heavy nuclear masses involved, the vibrational band shows a relatively compact and complex structure despite the simple linear geometric arrangement. Overall, rotational-vibrational lines of six isotopologues could be assigned and fitted permitting the derivation of an accurate selenium-carbon bond length.

Spectroscopic analysis has been greatly supported by high-level quantum-chemical calculations of the molecular structure and the harmonic and anharmonic force fields performed at the CCSD(T) level of theory. Scalar-relativistic effects on the molecular structure were also considered but found of little importance.

Keywords: Carbon subchalcogenide, Infrared spectroscopy, Laser ablation, CCSD(T) calculations

---

*This paper is dedicated to Prof. Dr. Stephan Schlemmer, on the occasion of his 60th birthday.

*Corresponding author
Email address: `sthorwirth@ph1.uni-koeln.de` (Sven Thorwirth)

1. Introduction

Over the years, binary carbon-rich clusters C_nX_m ($n > 1$, $m = 1, 2$) have been studied rather extensively both experimentally and theoretically due to their relevance for molecular structure and astrochemistry [see, e.g., Refs. 1, 2, and references therein]. Particularly because of the latter, those clusters comprising group 14 and 16 heteroatoms, i.e., oxygen, sulfur, and silicon, have received special attention from some high-resolution spectroscopists [3–19] and chains as complex as C_5S have been detected in space [20]. Considerably less is known for clusters containing heavier elements X. Selected systems (X= Ge, Ag, Cu, Ni,...) have been studied using matrix-isolation spectroscopic techniques [Refs. 21, 22, and references therein], however, very little data have been collected in the gas phase.

As far as binary carbon-rich clusters with heavy group 14 elements are concerned, only very recently high-resolution studies of several germanium-bearing clusters have been reported, one infrared observation of nonpolar GeC_3Ge [2] as well as two Fourier-transform microwave investigations of polar GeC_n ($n = 2, 4, 5, 6$) species [23, 24]. The situation is even less favorable with respect to clusters comprising carbon and heavy group 16 elements. For selenium, only an observation of the fundamental $J = 1 - 0$ rotational transition of diatomic CSe is found in the literature [25] and no heavier sub-chalcogenides C_nSe_m have been studied spectroscopically to date. So far, selected polyatomic carbon-selenium species were observed using mass spectrometry, targeted at C_nSe^- anions in which clusters with an even number of carbon atoms as heavy as $C_{10}Se^-$ were detected [26]. In organometallics, the C_3Se species has been used as a bridging ligand [27]. Some previous information on carbon-selenium species has been obtained from quantum-chemical calculations, albeit at rather modest levels of theory [26, 28–32].

The present paper reports the first high-resolution spectroscopic characterization of a polyatomic carbon-selenium cluster, linear SeC_3Se, accomplished by observation of its antisymmetric C-C-stretching mode ν_3 in the $5\,\mu$m range. The experimental work was complemented by high-level quantum chemical calculations performed at the coupled-cluster (CC) level of theory in combination with large basis sets to support the spectroscopic assignment. A possible influence of scalar-relativistic effects due to the presence of selenium has been evaluated. Additionally, the combination of experimental rotational constants of different isotopic species and calculated zero-point vibrational corrections permitted the determination of an accurate carbon-

selenium bond length in SeC_3Se.

2. Experimental setup

Carbon-selenium clusters were observed with the same experimental setup used in recent investigations of carbon-sulfur clusters [11, 12, 14]. Briefly, the spectrometer comprises a laser-ablation source (Nd:YAG laser frequency-tripled to operate at a wavelength of 355 nm, a repetition rate of 20 Hz, and a pulse energy of about 20 mJ) for cluster production, a widely tunable quantum cascade laser (QCL, Daylight Solutions) as a monochromatic radiation source and a Herriott-type multireflection cell aligned such to allow for 48 passes of the QCL beam. Sample rods were made by compressing 3:1 stoichiometric mixtures of graphite and selenium powder (Sigma-Aldrich) and a tiny amount of epoxy glue was added as binder to ensure mechanical stability. In a running experiment, following the laser pulse, the ablation products are guided through a reaction channel (10 mm, mounted on a Series 9 pulse valve) towards a slit exit (cross section 1 mm $\times$ 15 mm) using He buffer gas from a high-pressure reservoir (15 bar). At the nozzle exit, the cluster-seeded He-pulse expands adiabatically into a vacuum chamber kept at a background pressure of a few times 10^{-2} mbar resulting in typical cluster rotational temperatures of 20 to 40 K. A few mm downstream from the nozzle exit, the QCL beam intersects the cluster pulse perpendicularly to the direction of the traveling free jet, and the transmitted laser intensity is recorded as a function of wavenumber using liquid-N_2-cooled InSb detectors. Frequency calibration is performed using a wavemeter (Bristol Instruments), a Fabry-Perot étalon and standard calibration gases (OCS) resulting in a typical wavenumber accuracy of $\leq 10^{-3}$ cm^{-1}. Initially, rotational-vibrational transitions of the C_3 cluster [33] were used to optimize the experimental conditions. Later on, optimization was performed on selected transitions of SeC_3Se itself.

3. Quantum-chemical calculations

The high-resolution spectroscopic study of carbon-selenium clusters reported here was complemented with high-level quantum-chemical calculations. All calculations were performed at the CC singles and doubles (CCSD) level augmented by a perturbative treatment of triple excitations, CCSD(T), [34, 35] in combination with Dunning's correlation consistent polarized valence and polarized core-valence basis sets (frozen-core (fc) approximation:

3

cc-pVXZ; all-electron (ae) computations: cc-pwCVXZ, with X=T, Q) [36–39]) as well as analytic gradient techniques [40]. The theoretical best-estimate structure was calculated at the ae-CCSD(T)/cc-pwCVQZ level of theory, an approach shown previously to provide very accurate equilibrium structural parameters for molecules containing second-row, [e.g., Refs. 41–44] but also third-row main group elements such as germanium [2, 23, 24]. The structural parameters of SeC_3Se calculated at various levels of theory are summarized in Figure 1.

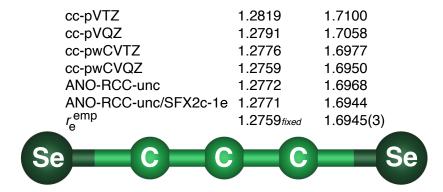|		
cc-pVTZ	1.2819	1.7100
cc-pVQZ	1.2791	1.7058
cc-pwCVTZ	1.2776	1.6977
cc-pwCVQZ	1.2759	1.6950
ANO-RCC-unc	1.2772	1.6968
ANO-RCC-unc/SFX2c-1e	1.2771	1.6944
r_e^{emp}	1.2759 *fixed*	1.6945(3)

Figure 1: Structural parameters of linear SeC_3Se calculated at the CCSD(T) level of theory using different basis sets as well as with and without consideration of scalar-relativistic effects (in Å). The semi-experimental (r_e^{emp}) Se−C bond length was determined while keeping the C−C distance fixed at the corresponding CCSD(T)/cc-pwCVQZ value. For further details, see text.

Vibrational effects were treated using second-order vibrational perturbation theory (VPT2) based on the formulas given in Ref. [45]. Harmonic and anharmonic force fields were calculated in the fc approximation at the CCSD(T) level of theory using basis sets as large as X = Q and analytic second-derivative techniques [46, 47] followed by numerical differentiation of the analytically computed Hessian with respect to the normal coordinates [48, 49] to obtain the required cubic and semidiagonal quartic anharmonic force fields [47, 49]. These calculations provide harmonic vibrational frequencies, centrifugal distortion and vibration-rotation interaction constants, zero-point vibrational corrections to the rotational constants ΔB_0, anharmonicity constants x_{ij} as well as fundamental vibrational frequencies (Table 1) and proved instrumental in the spectroscopic assignment and analysis.

As in the study of the GeC_3Ge cluster [2], the possible influence of scalar-relativistic effects on the molecular structure of SeC_3Se has been explored

Table 1: Vibrational wavenumbers and rotation-vibration interaction constants of $^{80}Se_2^{12}C_3$ (vibrational modes in cm^{-1}, α_i and q_i in MHz) as well as anharmonicity constants x_{ij} relative to the ν_3 mode (x_{3j}, in cm^{-1}).

Vib. mode	Calc.				Exp.	Para-meter	Calc.[a]	Exp.	x_{3j}[a]
	Harm.[a]	Anharm.[a]	Harm.[b]	Anharm.[c]					
$\nu_1(\sigma_g)$	1603	1582	1606	1585	$\cdots$	α_1	1.092	$\cdots$	-13.67
$\nu_2(\sigma_g)$	295	296	297	298	$\cdots$	α_2	0.157	$\cdots$	-1.39
$\nu_3(\sigma_u)$	2110	2070	2106	2066[d]	2057.2110(1)[e]	α_3	1.383	1.3656(8)[e]	-7.67
$\nu_4(\sigma_u)$	816	792	819	796	$\cdots$	α_4	0.729	$\cdots$	-3.90
$\nu_5(\pi_g)$	362	355	359	352	$\cdots$	α_5/q_5	$-0.417/0.026$	$\cdots$	-2.77
$\nu_6(\pi_u)$	481	408	460	387	$\cdots$	α_6/q_6	$-0.467/0.021$	$\cdots$	-11.41
$\nu_7(\pi_u)$	88	77	83	72	$\cdots$	α_7/q_7	$-0.709/0.094$	$\cdots$	-1.43

[a] fc-CCSD(T)/cc-pVTZ calculations.
[b] fc-CCSD(T)/cc-pVQZ calculations.
[c] Calculated from the fc-CCSD(T)/cc-pVQZ harmonic force field and anharmonic corrections calculated using VPT2 at the fc-CCSD(T)/cc-pVTZ level.
[d] Using a scaling factor derived from the ν_3 mode of isovalent SC$_3$S, 2066 cm^{-1} translates into a best-estimate value of 2056 cm^{-1}, see text.
[e] Gas-phase value (this work).

using the spin-free exact two-component scheme in its one-electron variant (SFX2c-1e) [50–54]. These calculations were performed with uncontracted versions of the ANO-RCC basis sets taken from Ref. [55].

All calculations were performed using the CFOUR program suite [56, 57]; a detailed review of the methods and strategies employed here can be found elsewhere [58].

4. Results and discussion

4.1. The ν_3 vibrational fundamental

Qualitatively, the appearance of the ν_3 band of SeC$_3$Se was expected to be rather similar to the corresponding band of GeC$_3$Ge [see Ref. 2]. Both clusters share similar structures and moments of inertia translating into small rotational constants of about 350 MHz and hence show rather compact rotation-vibration pattern. Also, both germanium and selenium have more than just one abundant stable isotope, germanium having three with natural abundances in excess of 20% and selenium having two, ^{80}Se (49.6%) and ^{78}Se (23.8%). Further selenium isotopes are found at abundances of 9.4% (^{76}Se), 8.7% (^{82}Se), and 7.6% (^{77}Se). Statistical distribution of these

isotopes over the two terminal positions in SeC_3Se gives rise to several abundant isotopic species and consequently was expected to result in quite some spectroscopic richness in the rotational structure of the vibrational band. As all abundant selenium isotopes as well as ^{12}C have no nuclear spin (i.e., $I = 0$; except for ^{77}Se which has $I = 1/2$), in addition, Bose-Einstein statistics will be at work for the symmetric species of $D_{\infty h}$ symmetry (e.g., $^{80}SeC_3^{80}Se$ and $^{78}SeC_3^{78}Se$)[1]. As a consequence, line spacing in these species will be approximately $4B$ whereas the presence of two different selenium isotopes in the same molecule will result in $C_{\infty v}$ symmetry and a regular $2B$ line spacing. A more detailed discussion about the effect and possible consequences of spin statistics in compact and partially overlapping spectra has been given in Ref. [2].

From the CCSD(T) calculations summarized in Table 1, the location of the ν_3 vibrational band of the 80–80 species was predicted at around $2066\,cm^{-1}$. However, by comparison with the calculations and experimental spectroscopic study of structurally closely related cumulenic chains such as SC_3S, SiC_3Si, and GeC_3Ge [2, 14, 16] the location of this band was expected to be shifted further to the red by several cm^{-1}. More quantitatively, using the calculated and experimental values of the ν_3 band of isovalent SC_3S for calibration purposes [14], a scaled (best estimate) value of $2056\,cm^{-1}$ is obtained for the 80–80 species. Interestingly, by tuning the QCL to this wavenumber while running laser ablation of a carbon-selenium rod in the very first experiment, an infrared spectroscopic signal was detected right away. Coarse tuning assays in this wavenumber range then revealed a spectroscopic pattern expected from the calculated SeC_3Se molecular parameters (Table 2) with the spin statistical effects. Finally, repeated fine tuning of the QCL over the frequency range from 2052 to $2060cm^{-1}$ and spectral averaging yielded the spectrum shown in Figure 2. The new band was only observed when target rods comprising both carbon and selenium were used in the experiment but not through ablation from a pure carbon target alone.

Spectroscopic assignment performed in the following commenced with the most abundant and prominent (parent) species, 80–80, and was guided by the calculated rotational constants (Table 2) assuming a $4B$ line spacing. As the

---

[1]For the sake of simplicity, in the text isotopic species of SeC_3Se will be specified by the corresponding selenium mass numbers only, e.g., $^{80}SeC_3^{80}Se$ will be denoted "80-80" and so forth.

Table 2: Molecular parameters for the ν_3 vibrational fundamental of $^{80}SeC_3^{80}Se$ and selected isotopic species (in MHz, unless otherwise noted). Calculated values are set in italics for the sake of clarity.

Parameter	^{80}SeCCCSe^{80}	^{78}SeCCCSe^{80}	^{78}SeCCCSe^{78}
$\tilde{\nu}_{\text{calc}}$ / cm$^{-1,a,b}$	*2069.97*	*2069.92*	*2069.98*
$\tilde{\nu}_{\text{calc,scaled}}$ / cm^{-1}	*n/a*	*2057.16*	*2057.22*
$\tilde{\nu}_{\text{exp}}$ / cm^{-1}	2057.21101(14)	2057.23484(10)	2057.21889(23)
$B_e{}^c$	*348.574*	*352.913*	*357.270*
$\Delta B_0{}^a$	*0.080*	*0.088*	*0.090*
$B_{0,\text{calc}}{}^d$	*348.487*	*352.825*	*357.180*
$B_{0,\text{calc,scaled}}{}^e$	*n/a*	*352.952*	*357.308*
B_0	348.605(22)	352.918(16)	357.201(62)
$\alpha_{3,\text{calc}}{}^a$	*1.383*	*1.401*	*1.418*
$\alpha_3{}^f$	1.3656(8)	1.4078(5)	1.4678(37)
$D_{e,\text{calc}} \times 10^{6,a}$	*2.073*	*2.125*	*2.177*
# lines	112	224	42
rms / cm^{-1}	0.0011	0.0012	0.0009
wrms^g	1.11	1.16	0.92
Abundance	*24.8%*	*23.6%*	*5.6%*
Relative Intensity	*1.0*	*0.48*	*0.23*

Parameter	^{82}SeCCCSe^{80}	^{77}SeCCCSe^{80}	^{76}SeCCCSe^{80}
$\tilde{\nu}_{\text{calc}}$ / cm$^{-1,a,b}$	*2069.97*	*2069.98*	*2069.96*
$\tilde{\nu}_{\text{calc,scaled}}$ / cm^{-1}	*2057.20*	*2057.21*	*2057.19*
$\tilde{\nu}_{\text{exp}}$ / cm^{-1}	2057.20463(21)	2057.20026(23)	2057.19919(20)
$B_e{}^c$	*344.422*	*355.153*	*357.454*
$\Delta B_0{}^a$	*0.085*	*0.089*	*0.090*
$B_{0,\text{calc}}{}^d$	*344.337*	*355.064*	*357.360*
$B_{0,\text{calc,scaled}}{}^e$	*344.461*	*355.191*	*357.488*
B_0	344.754(69)	355.120(67)	357.366(101)
$\alpha_{3,\text{calc}}{}^a$	*1.366*	*1.410*	*1.419*
$\alpha_3{}^f$	1.3576(40)	1.4030(42)	1.4697(53)
$D_{e,\text{calc}} \times 10^{6,a}$	*2.024*	*2.152*	*2.180*
# lines	58	49	58
rms / cm^{-1}	0.0014	0.0010	0.0009
wrms^g	1.37	1.00	0.93
Abundance	*8.7%*	*7.6%*	*9.2%*
Relative Intensity	*0.18*	*0.15*	*0.19*

[a] fc-CCSD(T)/cc-pVTZ.
[b] absolute accuracy 0.1 cm^{-1}.
[c] CCSD(T)/cc-pwCVTZ.
[d] $B_{0,\text{calc}} = B_e - \Delta B_0$.
[e] $X_{\text{calc,scaled}} = X_{\text{calc}} \times (X_{\text{exp}}/X_{\text{calc}})_{\text{SeCCCSe}}$.
[f] $\alpha_3 \approx B_0 - B_3$.
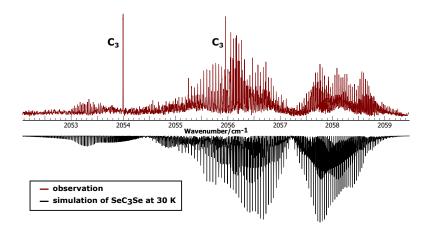[g] weighted rms, dimensionless.

Figure 2: The ν_3 vibrational band of SeC_3Se as observed in the gas phase *vs.* a simulation based on the best-fit parameters and a rotational temperature of 30K. In addition, two strong lines, $R(14)$ at $2054\,cm^{-1}$ and $R(16)$ at $2056\,cm^{-1}$, of the ν_3 mode of C_3 are prominently detected.

band center region at about $2057.2cm^{-1}$ is not free of spectroscopic signal and hence the first R- and P-branch lines, $R(0)$ and $P(2)$, were not detectable in a straightforward fashion, the initial assignment was performed by manually adjusting the band origin (while keeping B_0 and B_3 fixed at their calculated values) until good visual agreement between experiment and simulation was reached. In a second step, the band origin as well as B_0 and B_3 were then released in the fitting procedure and quantum number assignment to the experimental lines was adjusted such to best reproduce the calculated best-estimate rotational constants (Table 2). Overall, 118 rotational-vibrational transitions – ranging from P(112) to R(110) – were assigned to this isotopologue. The experimental transition wavenumbers were fit to within experimental accuracy by varying only three parameters using a standard linear rotor Hamiltonian: the vibrational band center, the ground-state rotational constant B_0, and the upper-state rotational constant B_3, or, alternatively, the corresponding rotation-vibration interaction parameter α_3. All spectroscopic data were analyzed using Pickett's SPFIT/SPCAT [59] as well as the Pgopher program [60] (see also the supplementary electronic material). In the following, despite a considerable number of (partially) overlapping lines and the resulting spectral complexity, five additional isotopic species were identified in the spectrum. Based on isotopic abundance and spin statistical

8

considerations, the ν_3 band of the 78–80 species is about half as intense as that of the 80–80 species (Table 2), followed by the 78–78 species at about one fourth and the 82–80, 76–80 and 77–80 species whose bands are expected to be weaker by factors of five to seven. Spectroscopic assignment of these species was performed based on their calculated band centers and lower and upper state rotational constants, B_0 and B_3, all of which were scaled further using correction factors derived from a comparison of the calculated and experimental parameters of the parent 80–80 species (see Table 2). As in case of GeC_3Ge [2], the vibrational wavenumber of the different isotopic species does hardly depend on the mass of the terminal heavy atoms, and from the CCSD(T)/cc-pVTZ force-field calculations the bands of all six species were expected to be centered within an interval of less than $0.1\,cm^{-1}$ (Table 2) and this renders theoretical predictions difficult. Despite the resultant spectroscopic interference and diminished line intensities relative to the parent species, more than 200 transitions were assigned to the 78–80 species, and still a few dozens of lines for all other species (see Table 2 and electronic supplementary material). As can be seen from the final molecular parameter sets summarized in Table 2, the empirical scaling approach is working well and the agreement between the scaled best estimates and experimentally parameters is good, to (much) better than $0.1\,cm^{-1}$ for the band centers and some $100\,kHz$ for the rotational constants. A $1\,cm^{-1}$ snippet of the experimental spectrum at $2056.6\,cm^{-1}$ along with a simulation based on the final parameter sets is shown in Figure 3. Taking account of the isotopic diversity and spectral density both show very good agreement.

4.2. Hot bands

The lower-wavenumber band "tail" visible in Figure 2 in the 2053 to $2055\,cm^{-1}$ region is reminiscent of the band contour also observed in the ν_3 band of SCCCS (see Figure 1 in Ref. [14]). These weaker spectroscopic features do not stem from any vibrational fundamental of an isotopic species but are hot band transitions associated with the ν_3 modes of the dominant isotopic species, 80–80 and 78–80, and originate from a lower-energy bending vibrational state. The offset estimated from simple visual inspection of the spectrum in Figure 2 is about $-3\,cm^{-1}$. Based on the calculated anharmonicity constants x_{3j} (Table 2) the bands are identified as the $\nu_3 + \nu_5 - \nu_5$ hot bands and, consequently, the lower state is the first excited ν_5 bending mode (calculated at $352cm^{-1}$ for the 80-80 species, Table 1). As can be deduced from Figure 4, spectroscopic assignment in this hot band is not
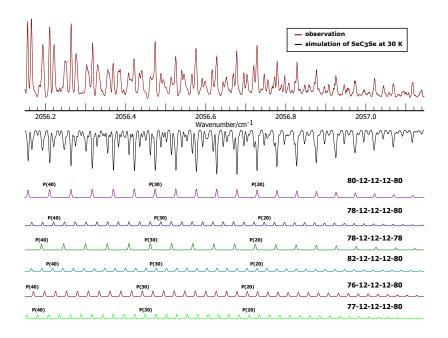
9

Figure 3: SeC$_3$Se ν_3 band close-up at 2056.6 cm^{-1} as observed in the present investigation. Detail of the experimental spectrum (maroon trace) obtained at 2056.6 cm^{-1} (top) and simulations of the ν_3 fundamentals of six SeC$_3$Se species as well as their superposition (black trace). Intensities of individual band simulations are not drawn to scale but to enhance clarity about location in the spectrum. All simulations are based on a rotational temperature of 30K.

straightforward due to severe line overlaps, a consequence of the overall isotopic richness and most likely also interference with other hot bands (such as $\nu_3 + \nu_7 - \nu_7$) which could however not be analyzed with confidence here. Guided by the calculated molecular parameters, the comparably clean region between 2053.0 and 2053.6 cm^{-1} in which the transitions of the dominating 80–80 and 78–80 species overlap constructively was used in a first assignment procedure and then additional features were added. Finally, 74 lines of the $\nu_3 + \nu_5 - \nu_5$ band have been assigned to the 78–80 species and 127 lines to 80–80. As the bending modes are doubly degenerate, ℓ-type doubling will result in a quasi-regular staggered $2B$ spacing in the hot band of the symmetric 80–80 species [cf., e.g, Ref. 61]. However, the ℓ-type doubling constant q_5 of SeC$_3$Se is very small (Table 1) so that line staggering of adjacent rotational-vibrational transitions is imperceptible in the spectrum. In fact, the effects of staggering are so small, that q_5 cannot be determined reliably in the fitting

procedure (cf. the situation in closely related SCCCS [14]). If released, q_5 amounts to $0.023(47)$ MHz which is in qualitative agreement with the calculation (Table 1). Consequently, ℓ-type doubling was also not resolved for the 78–80 species but both ℓ-components appear as one single line. The finally derived parameters sets are given in Table 3.
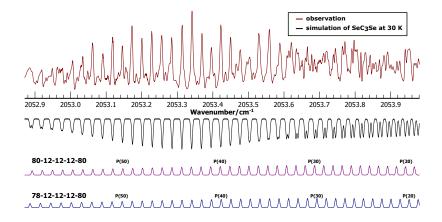

Figure 4: The $\nu_3 + \nu_5 - \nu_5$ hot-bands of ^{80}SeCCC^{80}Se and ^{78}SeCCC^{80}Se as observed here vs. a simulation based on the best-fit parameters and a temperature of 30K.

4.3. Molecular structure determination

The rotational constants derived from the observation of six isotopic species are, in principle, very useful for molecular structure determination. Unfortunately, the present study does not permit independent ascertainment of both unique structural parameters, $r_{\mathrm{Se-C}}$ and $r_{\mathrm{C-C}}$. Structure determination without constraints is hampered by the lack of ^{13}C data but most severely by the fact that the moment of inertia $I = \Sigma_i m_i r_i^2$ of SeC$_3$Se is dominated by the heavy masses and the terminal positions of the selenium atoms. As a consequence, $r_{\mathrm{Se-C}}$ and $r_{\mathrm{C-C}}$ cannot be determined simultaneously in a fully relaxed fitting procedure. In analogy to the strategy employed in case of GeC$_3$Ge [2], a fit of the carbon-heavy atom bond length $r_{\mathrm{Se-C}}$ was performed (using the equilibrium moments of inertia derived from $B_e = B_0 + \Delta B_0$, Table 2) while keeping $r_{\mathrm{C-C}}$ fixed at the theoretical best-estimate value of 1.2759 Å calculated at the CCSD(T)cc-pwCVQZ level of theory (Figure 1), a level known to yield highly accurate bond lengths for first-row but also second-row elements [see, e.g., Ref. 41]. From this, an

empirical equilibrium bond length r_{Se-C} of 1.6945(3) Å is derived (using the STRFIT program [62]), a value being in (virtually quantitative) agreement with the bond length calculated at the CCSD(T)/cc-pwCVQZ level of theory. It may be worthwhile to mention that rotational constants derived from alternative spectroscopic assignments ($\pm 2J$, as imposed by the spin statistical constraints of the 80–80 parent species) result in a significant bond length variation Δr_{Se-C} of ± 0.012 Å, a finding that also speaks very much in favor of the final spectroscopic assignment used in the analysis. Assuming a (very conservative) uncertainty in r_{C-C} of 10^{-3} Å a more conservative empirical value of $r_{Se-C} = 1.695(1)$ Å is obtained. Similar to the previous findings on Ge-C chains [2, 24], this result suggests that i) scalar-relativistic effects play a very minor role for the calculation of the Se-C bond length in Se_2C_3 (as deduced also from the CCSD(T)/ANO-RCC calculations highlighted in Figure 1) and ii) the CCSD(T)/cc-pwCVQZ level may offer a very favorable method-basis set balancing also for molecules harboring third-row main group elements.

The r_{Se-C} bond length in SeC_3Se is similar to the one found in linear triatomic OCSe, for which an empirical equilibrium value of 1.7098 Å has been determined from combined millimeter-/infrared high resolution spectroscopic studies [63]. For OCSe, an CCSD(T)/cc-pwCVQZ structural optimization performed here yields bond lengths of $r_{O-C} = 1.1529$ Å (vs. an experimental value of 1.1533 Å) and $r_{Se-C} = 1.7108$ Å. Again, very good agreement between the experimental and calculated carbon-selenium bond lengths is observed, lending independent support as to the adequacy of the CCSD(T)/cc-pwCVQZ level for the prediction of high-level structural parameters for carbon-rich selenium clusters in particular and probably even more generally for other selenium bearing species as well.

5. Conclusions

Laser ablation of carbon-selenium targets has led to the first high-resolution spectroscopic study of a polyatomic carbon-selenium cluster, linear SeC_3Se. Spectroscopic assignment of the dense ν_3 vibrational mode was made possible and facilitated by high-level quantum-chemical calculations performed at the CCSD(T) level of theory, despite the overall spectral complexity encountered in the band. Using rotational constants of six isotopic species permitted the derivation of an accurate carbon-selenium bond length which is found in very good agreement with the bond length calculated at the CCSD(T)/cc-

Table 3: Molecular parameters for the $\nu_3 + \nu_5 - \nu_5$ vibrational hot-band of ^{80}SeCCC^{80}Se and ^{78}SeCCC^{80}Se (in MHz, unless otherwise noted). Calculated values are set in italics for the sake of clarity.

Parameter	^{80}SeCCCSe^{80}	^{78}SeCCCSe^{80}
$\tilde{\nu}_{\mathrm{exp}}/\mathrm{cm}^{-1}$	2054.42441(13)	2054.44142(19)
$x^a_{35,\mathrm{calc}}/\mathrm{cm}^{-1}$	-2.77	-2.79
$x_{35,\mathrm{exp}}/\mathrm{cm}^{-1}$	$-2.78660(19)$	$-2.79342(21)$
$B_{5,\mathrm{calc}}{}^b$	349.022	353.335
B_5	348.831(40)	353.373(49)
$\alpha_3{}^c$	1.3656(8)	1.4078(5)
$\alpha_{\mathrm{hot}}{}^d$	1.3937(17)	1.4378(30)
# lines	127	74
rms / cm^{-1}	0.0013	0.0012
wrms^e	1.31	1.23

[a] fc-CCSD(T)/cc-pVTZ.
[b] $B_{5,\mathrm{calc}} = B_{0,\mathrm{exp}} - \alpha_{5,\mathrm{calc}}$.
[c] $\alpha_3 \approx B_0 - B_3$, see Table 2.
[d] $\alpha_{\mathrm{hot}} \approx B_5 - B_{3+5}$.
[e] weighted rms, dimensionless.

pwCVQZ level of theory. Scalar-relativistic effects were not found to have a significant impact on the molecular structure.

Based on the present findings, it would be very surprising if there were no other carbon-selenium clusters present in the laser ablation/free-jet expansion source. Indeed, the ν_1 mode of the closely related C_3Se cluster was detected recently in our laboratory [64] the analysis of which will be described in detail elsewhere. Longer carbon-selenium chains with more than three carbon atoms building the backbone might be detectable, too, but enlarging the chain-length will be accompanied by further increase of spectral complexity and line interference making spectroscopic assignment a very challenging task even when predictions from very high level quantum-chemical calculations are at hand. Ternary chalcogen carbon-rich clusters of the general form OC_nSe and SC_nSe might also be detectable by similar spectroscopic means in the infrared (and possibly by microwave pure rotational spectroscopy) to open an interesting field for the spectroscopic and structural study of medium-sized and heavy carbon-rich cluster systems.

Acknowledgments

Appendix A. Supplementary material

Supplementary data associated with this article can be found, in the online version, at XXX.

References

[1] S. Schlemmer, T. Giesen, H. Mutschke, C. Jäger (Eds.), Laboratory Astrochemistry, Wiley-VCH, Weinheim, Germany, 2015.

[2] S. Thorwirth, V. Lutter, A. Javadi Javed, J. Gauss, T. F. Giesen, Gas-Phase Spectroscopic Detection and Structural Elucidation of Carbon-Rich Group 14 Binary Clusters: Linear GeC_3Ge, J. Phys. Chem. A 120 (2016) 254–259.

[3] F. Holland, M. Winnewisser, G. Maier, H. P. Reisenauer, A. Ulrich, The high-resolution Fourier transform infrared spectrum of the ν_4 band system of OCCCCCO, J. Mol. Spectrosc. 130 (1988) 470–474.

[4] D. McNaughton, D. McGilvery, F. Shanks, High resolution FTIR analysis of the ν_1 band of tricarbon monoxide: Production of tricarbon monoxide and chloroacetylenes by pyrolysis of fumaroyl dichloride, J. Mol. Spectrosc. 149 (2) (1991) 458–473.

[5] T. Ogata, Y. Ohshima, Y. Endo, Rotational Spectra and Structures of Carbon Monoxides C_5O, C_7O, and C_9O, J. Am. Chem. Soc. 117 (12) (1995) 3593–3598.

[6] Y. Ohshima, Y. Endo, T. Ogata, Fourier-transform microwave spectroscopy of triplet carbon monoxides, C_2O, C_4O, C_6O, and C_8O, J. Chem. Phys. 102 (4) (1995) 1493–1500.

[7] R. Petry, S. Klee, M. Lock, B. Winnewisser, M. Winnewisser, Spherical mirror multipass system for FTIR jet spectroscopy: application to the rovibrationally resolved spectrum of OC_5O, J. Mol. Struct. 612 (2002) 369–381.

[8] L. Bizzocchi, C. Degli Esposti, L. Dore, Accurate rest frequencies for the submillimetre-wave lines of C_3O in ground and vibrationally excited states below $400\,cm^{-1}$, Astron. Astrophys. 492 (2008) 875–881.

[9] J. A. Tang, S. Saito, Microwave-Spectrum of the C_3S Molecule in the Vibrationally Excited-States of Bending Modes, ν_4 and ν_5, J. Mol. Spectrosc. 169 (1) (1995) 92–107.

[10] V. D. Gordon, M. C. McCarthy, A. J. Apponi, P. Thaddeus, Rotational spectra of sulfur-carbon chains. I. The radicals C_4S, C_5S, C_6S, C_7S, C_8S, and C_9S, Astrophys. J. Suppl. Ser. 134 (2001) 311–317.

[11] J. B. Dudek, T. Salomon, S. Fanghänel, S. Thorwirth, Carbon-sulfur chains: A high-resolution infrared and quantum-chemical study of C_3S and SC_7S, Int. J. Quantum Chem. 117 (2017) e25414.

[12] S. Thorwirth, T. Salomon, S. Fanghänel, J. R. Kozubal, J. B. Dudek, High-resolution infrared fingerprints of carbon-sulfur clusters: The ν_1 band of C_5S, Chem. Phys. Lett. 684 (2017) 262–266.

[13] B. A. McGuire, M.-A. Martin-Drumel, K. L. K. Lee, J. F. Stanton, C. A. Gottlieb, M. C. McCarthy, Vibrational satellites of C_2S, C_3S, and C_4S: microwave spectral taxonomy as a stepping stone to the millimeter-wave band, Phys. Chem. Chem. Phys. 20 (2018) 13870–13889.

[14] T. Salomon, J. B. Dudek, S. Bentley, S. Schlemmer, S. Thorwirth, A continued investigation of carbon subsulfide, SCCCS, at 5μm: New hot bands and isotopic species, J. Mol. Spectrosc. 356 (2019) 21–27.

[15] M. C. McCarthy, J. H. Baraban, P. B. Changala, J. F. Stanton, M.-A. Martin-Drumel, S. Thorwirth, C. A. Gottlieb, N. J. Reilly, Discovery of a missing link: detection and structure of the elusive disilicon carbide cluster, J. Phys. Chem. Lett. 6 (2015) 2107–2111.

[16] S. Thorwirth, J. Krieg, V. Lutter, I. Keppeler, S. Schlemmer, M. E. Harding, J. Vázquez, T. F. Giesen, High-resolution OPO spectroscopy

of Si_2C_3 at $5\mu m$: Observation of hot band transitions associated with ν_3, J. Mol. Spectrosc. 270 (2011) 75–78.

[17] V. D. Gordon, E. S. Nathan, A. J. Apponi, M. C. McCarthy, P. Thaddeus, P. Botschwina, Structures of the linear silicon carbides SiC_4 and SiC_6: Isotopic substitution and Ab Initio theory, J. Chem. Phys. 113 (2000) 5311–5320.

[18] M. C. McCarthy, A. J. Apponi, C. A. Gottlieb, P. Thaddeus, Laboratory detection of five new linear silicon carbides: SiC_3, SiC_5, SiC_6, SiC_7, and SiC_8, Astrophys. J. 538 (2000) 766–772.

[19] D. Witsch, V. Lutter, A. A. Breier, K. M. T. Yamada, G. W. Fuchs, J. Gauss, T. F. Giesen, Infrared spectroscopy of disilicon-carbide, Si_2C: The ν_3 fundamental band, J. Phys. Chem. A 123 (19) (2019) 4168–4177. `doi:10.1021/acs.jpca.9b01605`.

[20] M. Agúndez, J. Cernicharo, M. Guélin, New molecules in IRC+10216: confirmation of C_5S and tentative identification of MgCCH, NCCP, and SiH_3CN, Astron. Astrophys. 570 (2014) A45.

[21] E. Gonzalez, C. M. L. Rittby, W. R. M. Graham, Infrared observation of linear GeC_3 trapped in solid Ar, J. Chem. Phys. 130 (19) (2009) 194511.

[22] J. Szczepanski, Y. Wang, M. Vala, Copper-Carbon Cluster CuC_3: Structure, Infrared Frequencies, and Isotopic Scrambling, J. Phys. Chem. A 112 (21) (2008) 4778 – 4785. `doi:10.1021/jp801111m`.

[23] O. Zingsheim, M.-A. Martin-Drumel, S. Thorwirth, S. Schlemmer, C. A. Gottlieb, J. Gauss, M. C. McCarthy, Germanium Dicarbide: Evidence for a T-Shaped Ground State Structure, J. Phys. Chem. Lett. 8 (16) (2017) 3776–3781.

[24] K. L. K. Lee, S. Thorwirth, M.-A. Martin-Drumel, M. C. McCarthy, Generation and structural characterization of Ge carbides GeC_n(n= 4, 5, 6) by laser ablation, broadband rotational spectroscopy, and quantum chemistry, Phys. Chem. Chem. Phys. 21 (35) (2019) 18911 – 18919. `doi:10.1039/c9cp03607e`.

[25] J. McGurk, H. L. Tigelaar, S. L. Rock, C. L. Norris, W. H. Flygare, Detection, assignment of the microwave spectrum and the molecular

Stark and Zeeman effects in CSe, and the Zeeman effect and sign of the dipole moment in CS, J. Chem. Phys. 58 (1973) 1420–1424.

[26] H.-Y. Wang, R.-B. Huang, H. Chen, M.-H. Lin, L.-S. Zheng, Studies of Linear C_nSe^- ($1 \leq n \leq 11$) Clusters Produced from Laser Ablation: Collision-Induced Dissociation and ab Initio Calculations, J. Phys. Chem. A 105 (2001) 4653–4659.

[27] A. F. Hill, R. A. Manzano, M. Sharma, J. S. Ward, Selenoxopropadienylidene (CCCSe) as a Bridging Ligand, Organometallics 34 (2014) 361–365.

[28] W. Wu, J. Zhang, Z. Cao, CASPT2 studies on the electronic spectra of linear heteroatom-containing carbon chain anions C_4O^-, C_4S^- and C_4Se^-, J. Mol. Struct.: THEOCHEM 765 (2006) 137–141.

[29] A. Bundhun, P. Ramasami, Density functional theory study of the carbon chains C_nX, C_nX^+ and C_nX^- (X = O and Se; n =1–10), Eur. Phys. J. D 57 (2010) 355–364.

[30] E. F. Villanueva, P. Redondo, V. M. Rayón, C. Barrientos, A. Largo, Small carbides of third-row main group elements: structure and bonding in C_3X compounds (X = K–Br), Phys. Chem. Chem. Phys. 14 (2012) 14923–14932.

[31] Z. Zhang, L. Pu, X. Zhao, Q.-s. Li, R. B. King, Differences between carbon suboxide and its heavier congeners as ligands in transition metal complexes: a theoretical study, New J. Chem. 40 (2016) 9486–9493.

[32] L. Pu, X. Zhao, Z. Zhang, R. B. King, Heavier Carbon Subchalcogenides as C_3 Sources for Tungsten-Capped Cumulenes: A Theoretical Study, Inorg. Chem. 56 (2017) 5567–5576.

[33] K. Matsamura, H. Kanamori, K. Kawaguchi, E. Hirota, Infrared diode laser kinetic spectroscopy of the ν_3 band of C_3, J. Chem. Phys. 89 (1988) 3491–3494.

[34] K. Raghavachari, G. W. Trucks, J. A. Pople, M. Head-Gordon, A 5th-order perturbation comparison of electron correlation theories, Chem. Phys. Lett. 157 (1989) 479–483.

[35] I. Shavitt, R. J. Bartlett, Many-Body Methods in Chemistry and Physics: MBPT and Coupled-Cluster Theory, Cambridge University Press, Cambridge, U.K., 2009.

[36] T. H. Dunning, Gaussian basis sets for use in correlated molecular calculations .1. The atoms boron through neon and hydrogen, J. Chem. Phys. 90 (1989) 1007–1023.

[37] A. K. Wilson, D. E. Woon, K. A. Peterson, T. H. Dunning, Gaussian basis sets for use in correlated molecular calculations. ix. the atoms gallium through krypton, J. Chem. Phys. 110 (16) (1999) 7667–7676.

[38] K. A. Peterson, T. H. Dunning, Accurate correlation consistent basis sets for molecular core-valence correlation effects: The second row atoms Al-Ar and the first row atoms B-Ne revisited, J. Chem. Phys. 117 (2002) 10548–10560.

[39] N. B. Balabanov, K. A. Peterson, Systematically convergent basis sets for transition metals. I. All-electron correlation consistent basis sets for the 3d elements Sc–Zn, J. Chem. Phys. 123 (2005) 064107.

[40] J. D. Watts, J. Gauss, R. J. Bartlett, Open-shell analytical energy gradients for triple excitation many-body, coupled-cluster methods - MBPT(4), CCSD+T(CCSD), CCSD(T), and QCISD(T), Chem. Phys. Lett. 200 (1992) 1–7.

[41] S. Coriani, D. Marcheson, J. Gauss, C. Hättig, T. Helgaker, P. Jørgensen, The accuracy of ab initio molecular geometries for systems containing second-row atoms, J. Chem. Phys. 123 (2005) 184107–1–184107–12.

[42] S. Thorwirth, M. E. Harding, Coupled-cluster calculations of C_2H_2Si and CNHSi structural isomers, J. Chem. Phys. 130 (2009) 214303.

[43] M. C. McCarthy, C. A. Gottlieb, P. Thaddeus, S. Thorwirth, J. Gauss, Rotational spectra and equilibrium structures of H_2SiS and Si_2S, J. Chem. Phys. 134 (2011) 034306.

[44] L. A. Mück, S. Thorwirth, J. Gauss, The semi-experimental equilibrium structures of AlCCH and AlNC, J. Mol. Spectrosc. 311 (2015) 49–53.

18

[45] I. M. Mills, Vibration-Rotation Structure in Asymmetric- and Symmetric-Top Molecules, Academic Press, New York, 1972, pp. 115–140.

[46] J. Gauss, J. F. Stanton, Analytic CCSD(T) second derivatives, Chem. Phys. Lett. 276 (1997) 70–77.

[47] J. F. Stanton, J. Gauss, Analytic second derivatives in high-order many-body perturbation and coupled-cluster theories: computational considerations and applications, Int. Rev. Phys. Chem. 19 (2000) 61–95.

[48] W. Schneider, W. Thiel, Anharmonic force fields from analytic second derivatives: Method and application to methyl bromide, Chem. Phys. Lett. 157 (1989) 367–373.

[49] J. F. Stanton, C. L. Lopreore, J. Gauss, The equilibrium structure and fundamental vibrational frequencies of dioxirane, J. Chem. Phys. 108 (1998) 7190–7196.

[50] K. Dyall, Interfacing relativistic and nonrelativistic methods. IV. One- and two-electron scalar approximations, J. Chem. Phys. 115 (2001) 9136–9143.

[51] W. Kutzelnigg, W. J. Liu, Quasirelativistic theory equivalent to fully relativistic theory, J. Chem. Phys. 123 (2005) 241102.

[52] W. Liu, D. Peng, Exact two-component Hamiltonians revisited, J. Chem. Phys. 131 (2009) 031104.

[53] M. Ilias, T. Saue, An infinite-order two-component relativistic Hamiltonian by a simple one-step transformation, J. Chem. Phys. 126 (2007) 064102.

[54] L. Cheng, J. Gauss, Analytic energy gradients for the spin-free exact two-component theory using an exact block diagonalization for the one-electron Dirac Hamiltonian, J. Chem. Phys. 135 (2011) 084114.

[55] B. Roos, V. Veryazov, P. Widmark, Relativistic atomic natural orbital type basis sets for the alkaline and alkaline-earth atoms applied to the ground-state potentials for the corresponding dimers, Theor. Chem. Acc. 111 (2004) 345–351.

[56] D. A. Matthews, L. Cheng, M. E. Harding, F. Lipparini, S. Stopkowicz, T.-C. Jagau, P. G. Szalay, J. Gauss, J. F. Stanton, Coupled-cluster techniques for computational chemistry: The CFOUR program package, J. Chem. Phys. 152 (2020) 214108.

[57] M. E. Harding, T. Metzroth, J. Gauss, A. A. Auer, Parallel calculation of CCSD and CCSD(T) analytic first and second derivatives, J. Chem. Theory Comput. 4 (2008) 64–74.

[58] C. Puzzarini, J. F. Stanton, J. Gauss, Quantum-chemical calculation of spectroscopic parameters for rotational spectroscopy, Int. Rev. Phys. Chem. 29 (2010) 273–367.

[59] H. M. Pickett, The fitting and prediction of vibration-rotation spectra with spin interactions, J. Mol. Spectrosc. 148 (1991) 371–377.

[60] C. M. Western, PGOPHER: A program for simulating rotational, vibrational and electronic spectra, J. Quant. Spectrosc. Radiat. Transfer. 186 (2016) 221–241.

[61] P. Neubauer-Guenther, T. F. Giesen, S. Schlemmer, K. M. T. Yamada, The high resolution infrared spectra of the linear carbon cluster C_7: the ν_4 stretching fundamental band and associated hot bands, J. Chem. Phys. 127 (2007) 014313.

[62] Z. Kisiel, Least-squares mass-dependence molecular structures for selected weakly bound intermolecular clusters, J. Mol. Spectrosc. 218 (2003) 58–67.

[63] M. LeGuennec, G. Wlodarczak, G.Darczak, J. Demaison, H. Bürger, M. Litz, H. Willner, Millimeterwave and High-Resolution Infrared Spectra of OCSe: Determination of Its Structure, J. Mol. Spectrosc. 157 (1993) 419–446.

[64] T. Salomon, Y. Chernyak, J. B. Dudek, J. Gauss, S. Schlemmer, S. Thorwirth, High-resolution infrared spectroscopy of carbon-selenium chains: SeC_3Se and C_3Se, in: International Symposium on Molecular Spectroscopy, 74th meeting, Champaign-Urbana, IL, U.S.A., June 17-21, Talk TC06, 2019.